Inhibition of autophagy enhanced cobalt chloride-induced apoptosis in rat alveolar type II epithelial cells

YAN YU*, WANTING LI*, LIQIN REN*, CHUNYAN YANG*, DONGZE LI, XIN HAN, YEYING SUN, CHANGJUN LV and FANG HAN

Medicine and Pharmacy Research Center, Binzhou Medical University, Yantai, Shandong 264003, P.R. China

Received November 7, 2017; Accepted April 10, 2018

DOI: 10.3892/mmr.2018.9209

Abstract. Hypoxia is a type of cellular stress that may result in apoptosis and autophagy. The molecular mechanisms underlying the association between autophagy and apoptosis remain unclear, particularly in hypoxic conditions. Transmission electron microscope, AO-PI staining, flow cytometry and western blot were used to examine the crosstalk between autophagy and apoptosis in hypoxic conditions. Rat alveolar type II epithelial RLE-6TN cells were cultured in a long-term hypoxic environment established by cobalt (II) chloride. It was demonstrated that autophagy and apoptosis occurred in RLE-6TN cells under hypoxic conditions. Treatment of RLE-6TN cells with the autophagy inhibitor 3-methyladenine increased the generation of reactive oxygen species, mitochondrial damage and hypoxia-induced apoptosis. The expression of caspases, particularly caspase-9, increased and may have participated in these processes. The data indicated that the inhibition of autophagy enhanced apoptosis through the mitochondria-mediated intrinsic pathway. These findings provide important insight into the molecular mechanism of autophagy and apoptosis crosstalk. This may provide new insights into pulmonary disease surveillance, diagnosis and treatment.

Introduction

Hypoxia results in pathophysiological damage to various cells and tissues. Cells possess a powerful regulatory system involving hypoxia-inducible factors (HIFs) that respond to hypoxic stress (1-3). HIF-1α regulates metabolic adaptation to hypoxia and activates multiple target genes, including vascular endothelial growth factor, erythropoietin and nuclear factor-κB under hypoxic conditions (4). Furthermore, HIF-1α has been implicated as a co-regulator of autophagy activation and also participates in apoptosis (5).

Autophagy protects cells from various damaging factors, including hypoxia or starvation and maintains intracellular stability (6). It has been demonstrated that autophagy is closely associated with apoptosis under hypoxic condition (5). Apoptosis is a type of programmed cell death which is triggered by intrinsic or extrinsic signals (7). Hypoxia and cobalt (II) chloride ($CoCl_2$) treatment activate autophagy through the target genes induced by HIF, such as mechanistic target of rapamycin (2) and correlate with the expression of certain pro-apoptotic factors, including caspase-9 and caspase-3 (8,9). These results suggest that autophagy and apoptosis often occur in parallel following $CoCl_2$ treatment, with autophagy typically occurring prior to apoptosis. The important role of autophagy may be associated with the regulation of apoptosis. It has been reported that autophagy attenuates cellular injury by inhibiting the induction of apoptosis (10).

Autophagy and apoptosis may serve pivotal roles in neurodegenerative disease (11). A previous report revealed that autophagy serves a dual role, by exhibiting a protective role for cell survival, but autophagy may also promote apoptosis associated with various lung diseases, including chronic obstructive pulmonary disease, idiopathic pulmonary fibrosis and sepsis (12). However, the molecular mechanism of crosstalk between autophagy and apoptosis remains unclear. In the present study, the association between autophagy and apoptosis induced by long-term $CoCl_2$ treatment in RLE-6TN cells was investigated. The results suggested that autophagy provided a survival strategy for RLE-6TN cells via apoptosis inhibition. The present study may aid in elucidating the underlying molecular mechanism of autophagy and apoptosis interaction in a hypoxic environment, which may contribute to the development of novel treatments for the therapy of lung diseases.

Materials and methods

Reagents and antibodies. $CoCl_2$, 2,7-dichlorodihyfluorescein diacetate (DCFH-DA), Tris, glycine, Tween-20, SDS, acridine orange (AO), propidium iodide (PI), anti-microtubule associated

Correspondence to: Dr Changjun Lv or Dr Fang Han, Medicine and Pharmacy Research Center, Binzhou Medical University, 346 Guanhai Road, Yantai, Shandong 264003, P.R. China
E-mail: lucky_lcj@sina.com
E-mail: hanfangtuandui@163.com

*Contributed equally

Key words: hypoxia, autophagy, apoptosis, 3-methyladenine, caspase

proteins 1A/1B light chain 3B (LC3I/II; cat. no. L7543) were purchased from Sigma-Aldrich (Merck KGaA, Darmstadt, Germany). Trypsin-EDTA was obtained from Thermo Fisher Scientific, Inc. (Waltham, MA, USA). Trypsin solution without EDTA was purchased from Beyotime Institute of Biotechnology (Hangzhou, China). The Annexin V-fluorescein isothiocyanate (FITC)/PI apoptosis detection kit was purchased from BD Biosciences (San Jose, CA, USA). Primary antibodies were purchased from CST Biological Reagents, Co., Ltd. (Shanghai, China) or Abcam (Cambridge, UK). Secondary antibodies were purchased from OriGene Technologies, Inc. (Beijing, China). All other chemicals were obtained from Sigma-Aldrich (Merck KGaA). Radioimmunoprecipitation assay (RIPA) lysis buffer and phenylmethylsulfonyl fluoride (PMSF) were purchased from Beijing Solarbio Science & Technology Co., Ltd. (Beijing, China).

Cell culture and treatments. RLE-6TN cell line was provided by Binzhou Medical University (Yantai, China). Cells were cultured in RPIM-1640 medium (Hyclone; GE Healthcare Life Sciences, Logan, UT, USA) supplemented with 10% fetal bovine serum (Hyclone; GE Healthcare Life Sciences) and maintained at 37˚C in a humidified atmosphere with 5% CO_2. Hypoxia was established with $CoCl_2$ (100 μM) as previously described (13,14). The concentration of the autophagy inhibitor 3-methyladenine (3-MA; 1.5 mM) was determined by creating a dose-response curve in a preliminary experiment (data not shown). RLE-6TN cells were plated in 10-cm diameter plastic dish until 70-80% confluence was attained. Cells were treated with or without $CoCl_2$ and/or 3-MA for 1, 3, 5 and 7 days at 37˚C.

Transmission electron microscopy (TEM). For ultrastructural observation, cells were fixed with 2.5% paraformaldehyde and 2% glutaraldehyde in 0.1 M phosphate buffer (pH 7.4) for 2 h at 4˚C. Cells were subsequently post-fixed at 4˚C with 1% osmium tetroxide for 1 h and dehydration was performed using 50, 70, 80, 95 and 100 ethanol, and 100% acetone sequentially every 15 min and embedded in Epon 812 resin at 37˚C for 12 h, at 45˚C for 12 h and 60˚C for 36 h. Following this, cells were cut into ultrathin sections, imposed on a copper grid and stained with uranyl acetate for 30 min and led citrate for 10 min at room temperature. Observations and photographs were obtained using a JEOL JEM 1,011 microscope with a MORADA camera (JEOL Ltd., Tokyo, Japan).

Reactive oxygen species (ROS) assay. DCFH-DA was used to detect ROS levels. DCFH-DA converts into the highly fluorescent DCF upon oxidation by ROS. Cultured RLE-6TN cells were plated at a density of $1x10^5$ cells/ml in 6-well plates and incubated with RPIM-1640 medium supplemented with 10% fetal bovine serum overnight at 37˚C. DCFH-DA working solution was added directly to the medium to reach 20 μM and incubated at 37˚C for 30 min. Cells were subsequently washed with PBS three times and visualized with a fluorescence microscope (excitation wavelength, 488 nm; magnification, x200).

AO/PI double staining. RLE-6TN cells (80-90% confluence) were plated in 24 well-plates on a glass slide at 37˚C for 24 h. Following incubation, the cells in control group and treated RLE-6TN cells were harvested and washed twice with PBS. Glass slides were subsequently stained with 10 μg/ml of AO/PI for 5 min in the dark at 37˚C, followed by washing with PBS three times. Stained cells were observed under a fluorescence microscope (excitation wavelength, 488 nm; magnification, x200).

Annexin V/PI apoptosis assay. To analyze apoptosis, the FITC Annexin V Apoptosis Detection kit (BD Biosciences) was used according to the manufacturer's protocols. Treated cells ($1x10^6$) were washed with binding buffer of the aforementioned kit and resuspended in 100 μl binding buffer containing 5 μl FITC and 5 μl PI. After 15 min of incubation at room temperature in the dark, 400 μl binding buffer was added and the apoptotic rate of cells was analyzed with a flow cytometer (FACSDiva Software 6.0, BD Biosciences).

Western blot analysis. RLE-6TN cells were lysed in ice-cold RIPA lysis buffer (1 ml RIPA; 10 μl PMSF) for 30 min. Protein concentration was determined with a bicinchoninic acid protein assay kit and proteins (50 μg/lane) were separated by 12 and 15% SDS-PAGE and transferred to polyvinylidene fluoride membranes. Membranes were blocked at room temperature for 2 h with 5% skimmed milk in Tris-buffered saline with 0.1% Tween-20 (cat. no. ST825; Beyotime Institute of Biotechnology) and subsequently probed with the following antibodies at 4˚C overnight: Anti-β-actin antibody (1:2,000; cat. no. bs-0061R; BIOSS; Beijing, China), Anti-HIF-1α (1:1,000; cat. no. 14179; CST Biological Reagents Co., Ltd.), anti-LC3I/II (1:1,000; cat. no. L7543; Sigma-Aldrich; Merck KGaA), anti-cleaved caspase-9 (1:300; cat. no. ab2325; Abcam), anti-caspase-8 (1:1,000; cat. no. ab25901; Abcam), anti-cleaved caspase-3 (1:1,000; cat. no. 9664; CST Biological Reagents Co., Ltd.). Following this, membranes were incubated with horseradish peroxidase-conjugated goat anti-rabbit IgG (1:5,000; ZB2301; OriGene Technologies, Inc.) antibody for 1 h at room temperature. Proteins were visualized with an enhanced chemiluminescence substrate kit (Clinx Science Instruments Co., Ltd., Shanghai, China) and standard X-ray film development (ChemiScope 3,300 mini; Clinx Science Instruments Co., Ltd.). Results were quantified with ImageJ software v1.48 (National Institutes of Health, Bethesda, MD, USA) and processed using Adobe Photoshop CS5 (Adobe Systems, Inc., San Jose, CA, USA).

Statistical analysis. All experiments were performed at least three times. The data were expressed as the mean ± standard deviation. Statistical analyses were performed using SPSS 17.0 (SPSS, Inc., Chicago, IL, USA). Data were analyzed by one-way analysis of variance followed by Fisher's least significant difference. $P<0.05$ was considered to indicate a statistically significant difference.

Results

Hypoxia induces organelle impairment and autophagosome generation. Previous studies have demonstrated that cancer cells adapt to hypoxia or nutrient deprivation through autophagy activation (15,16). In the present study, TEM was used to observe the ultrastructure following $CoCl_2$ treatment

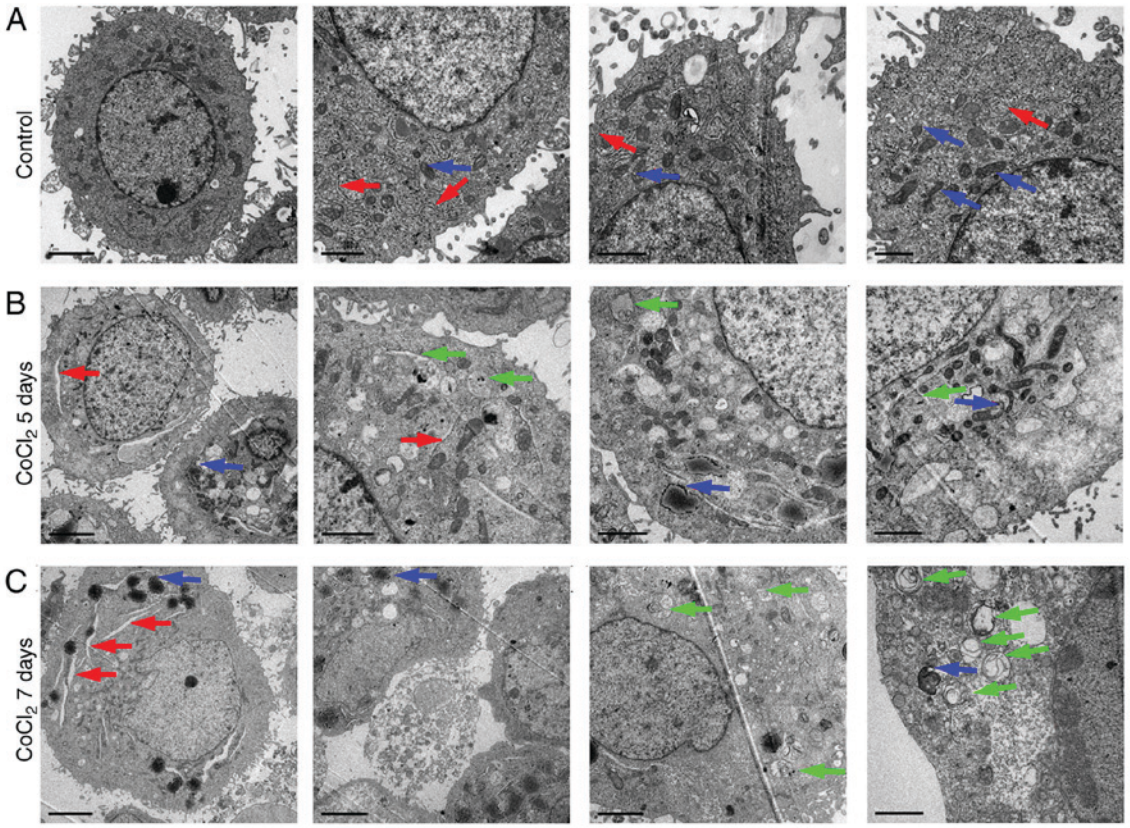

Figure 1. Hypoxia-induced autophagy in RLE-6TN cells. Representative TEM images of the morphological and subcellular structure of different groups. (A) Untreated RLE-6TN cells were observed by TEM. The endoplasmic reticulum and mitochondria of control group were normal. (B and C) Swollen endoplasmic reticulum and mitochondria were observed in $CoCl_2$ treatment group. In addition, autophagosomes in the cytoplasm also were observed in the $CoCl_2$ treatment group. Red, blue and green arrowheads indicate the endoplasmic reticulum, mitochondria and autophagosomes, respectively. TEM, transmission electron microscopy. $CoCl_2$, cobalt (II) chloride. Scale bar, 2 μm.

in RLE-6TN cells (Fig. 1). Compared with untreated cells (Fig. 1A), numerous autophagosomes consisting of double membranes were observed in the $CoCl_2$-treated RLE-6TN cells on days 5 and 7 (Fig. 1B and C, respectively). No notable autophagosomes were observed after 1 and 3 days following treatment with $CoCl_2$ (data not shown). Cytoplasmic material and/or membrane vesicles were encapsulated in the autophagosomes. Furthermore, swollen endoplasmic reticuli and damaged mitochondria were also observed following $CoCl_2$ treatment (Fig. 1B and C). These results indicated that 100 μm $CoCl_2$ treatment resulted in severe organelle impairment and induced autophagy generation.

3-MA enhances apoptosis in hypoxic conditions. Apoptosis is characterized by distinct morphological features and energy-dependent biochemical mechanisms. Cell pyknosis, cell shrinkage and chromatin condensation typically occur in early apoptosis (17,18). Budding in late apoptosis is a result of extensive blebbing of the plasma membrane to form apoptotic bodies containing tightly packed organelles (19). In the present study, fluorescence microscopy was used to detect the morphological changes in RLE-6TN cells following $CoCl_2$ and/or 3-MA treatment for 1, 3, 5 and 7 days (Fig. 2A-D). $CoCl_2$ treatment resulted in a reddish-orange color in nucleus due to the binding of PI to denatured DNA. Lysosomes in the cytoplasm were stained orange by PI in Fig. 2. This abundance of apoptotic cells, as indicated by arrows, was more prominent as the incubation time increased. 3-MA markedly increased the number reddish-orange stained nuclei in 100 μm $CoCl_2$-treated cells (Fig. 2D). These results indicated that autophagy was associated with apoptosis in RLE-6TN cells in hypoxic conditions and that autophagy may have a protective role in a hypoxic environment.

The apoptotic effect induced by $CoCl_2$ was further confirmed by flow cytometry (Fig. 3A). The results demonstrated that $CoCl_2$ treatment significantly increased in the percentage of cells in upper right and lower right quadrants (early and late apoptotic cells, respectively) after 3 days of treatment. 3-MA significantly increased $CoCl_2$-induced apoptosis in RLE-6TN cells at days 5 and 7 ($P<0.05$; Fig. 3B).

Taken together, these results suggested that the inhibition of autophagy strongly accelerated the process of apoptosis.

Inhibiting autophagy increases mitochondrial damage. Mitochondria have a double-membrane structure and are key organelles for the production of energy (20). In addition, mitochondria regulate cellular redox signaling pathways and programmed cell death (20). In order to explore the effect of 3-MA in $CoCl_2$-treated mitochondria, TEM was used to examine the mitochondrial ultrastructure. As presented in Fig. 4, swollen mitochondria were observed following $CoCl_2$ treatment at day 7, compared with the control. Mitochondrial damage was not notably observed on day 3; however, more notable damage was reported on day 5 (data not shown). Notably, more marked

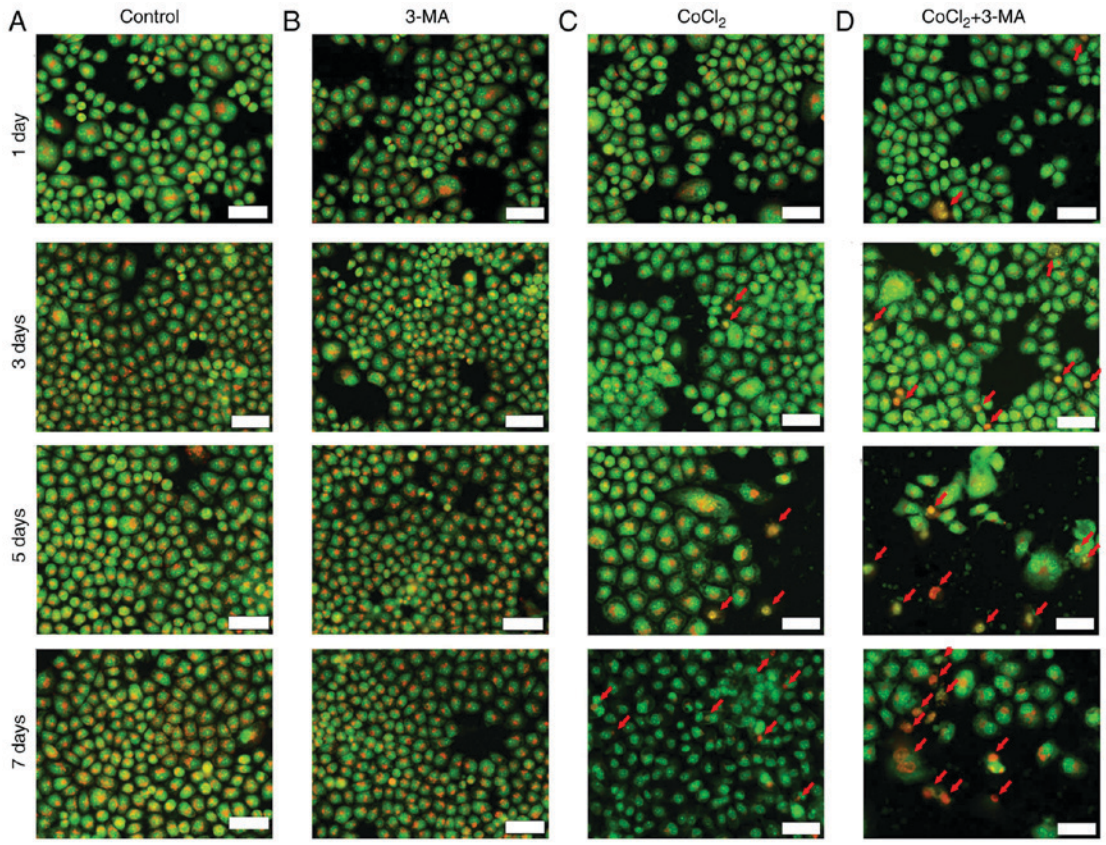

Figure 2. Apoptosis was measured by acridine orange/propidium iodide double staining in RLE-6TN cells. (A) No apoptotic cells were found in control group and the (B) 3-MA group. (C) Apoptosis was observed at days 3, 5 and 7 in the $CoCl_2$ treatment group. (D) Apoptosis occurred earlier at day 1 following 3-MA treatment in combination with $CoCl_2$ in RLE-6TN cells. Arrowheads indicate the apoptotic cells. $CoCl_2$, cobalt (II) chloride; 3-MA, 3-methyladenine. Scale bar, 50 μm. Magnification, x200.

mitochondrial damage was observed in the $CoCl_2$ + 3-MA group, including severely swollen mitochondria, double-membrane destruction and loss of normal morphology, suggesting that the inhibition of autophagy increased the extent of mitochondrial damage in RLE-6TN cells under hypoxic conditions.

Inhibiting autophagy increases the production of ROS. ROS are critical regulators in various cellular processes, including autophagy and apoptosis (21,22). Mitochondria are a major source of ROS in cells (23). A fluorescent probe, DCFH-DA, was used to detect the generation of ROS. As presented in Fig. 5, DCFH-DA fluorescence was markedly increased following $CoCl_2$ and 3-MA treatment, compared with $CoCl_2$ treatment alone. The results revealed that the inhibition of autophagy with 3-MA increased ROS generation and increased the rate of apoptosis in RLE-6TN cells. These results indicated that autophagy may prevent cell impairment in a hypoxic environment.

3-MA upregulates the expression of caspases in hypoxic conditions. Autophagy and apoptosis are two important catabolic processes (24) and the relationship between them remains unclear. In order to explore the complex crosstalk between autophagy and apoptosis, the expression of several proteins associated with these processes in response to hypoxia was investigated. As presented in Fig. 6, HIF-1α expression was significantly upregulated on days 2, 3, 5 and 7 after treatment with $CoCl_2$. This data indicated that the hypoxia model was successfully conducted in our study. In addition, cleaved-caspase-9, cleaved-caspase-8, cleaved-caspase-3, LC3II/I exhibited increasing trend; the expression levels were significantly higher on days 5 and 7 compared with in the control. Notably, 3 days following $CoCl_2$ treatment, cleaved-caspase-8 also significantly increased. Following 3-MA treatment (Fig. 7), the expression levels of LC3II/LCI, key proteins in autophagy, did not exhibit significant alterations under hypoxic conditions compared with in the control. By contrast, expression levels of cleaved caspase-9 and cleaved caspase-3 were significantly increased, particularly on days 5 and 7. Compared with cleaved-caspase-9 and cleaved-caspase-3, the expression level of cleaved caspase-8 appeared to be upregulated to a lesser degree. These results indicated that autophagy and apoptosis occurred in RLE-6TN cells under hypoxic conditions. Inhibition of autophagy may have accelerated apoptosis, predominantly through caspase-9-mediated intrinsic pathways in RLE-6TN cells in a chronic hypoxic environment.

Discussion

Cellular stress stimuli, such as hypoxia, may induce cells to exhibit their dual role (25). Cells may activate cytoprotective pathways, such as autophagy, to favor survival until the stress is resolved. Conversely, cells also may undergo programmed cell

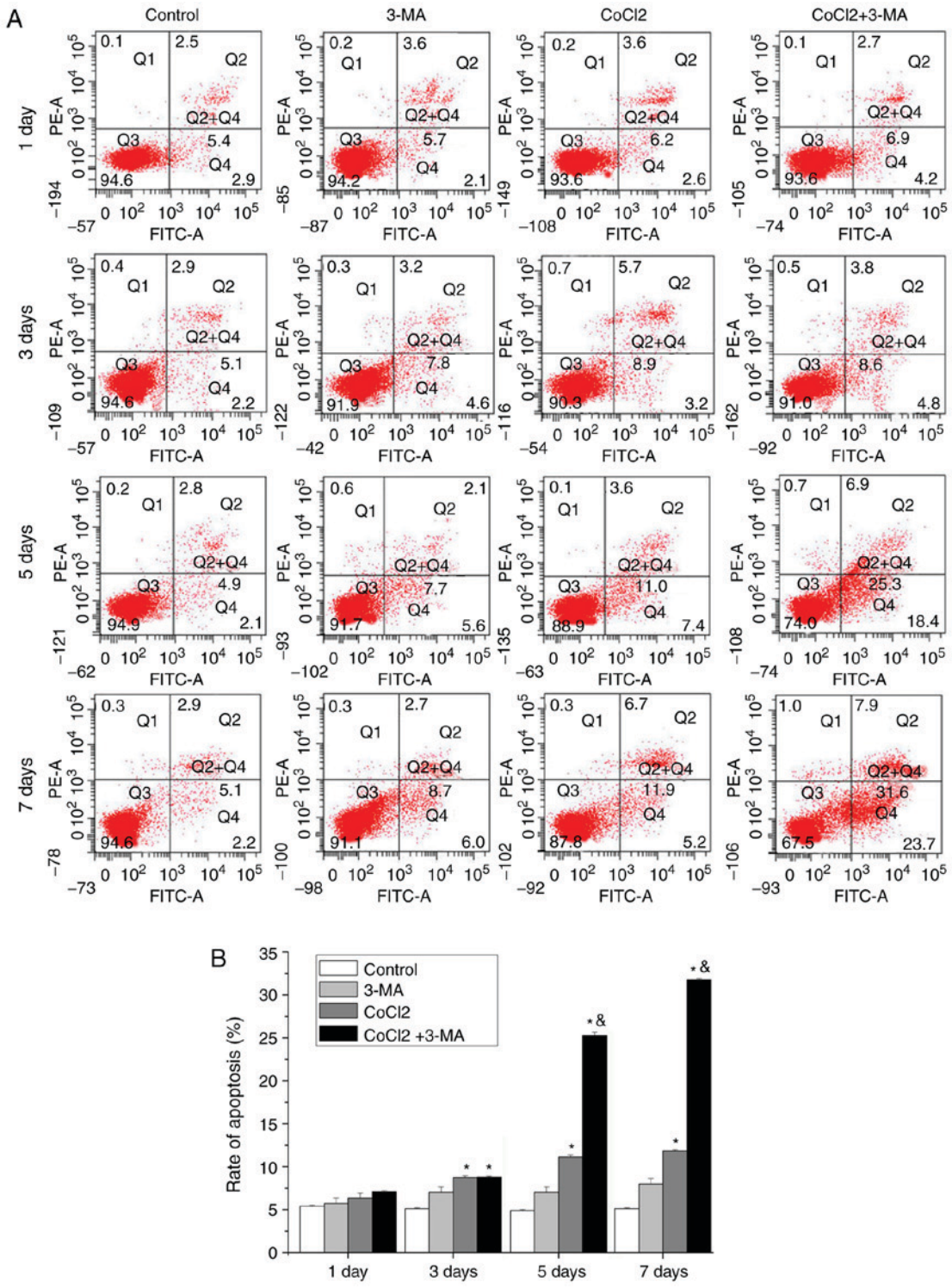

Figure 3. 3-MA significantly increased the apoptotic rate under hypoxic conditions. Apoptosis was detected by a Annexin V-fluorescein isothiocyanate assay. (A) Flow cytometry analysis of apoptosis. Q2 represented the early apoptotic cells. Q4 represented the late apoptotic cells. Apoptotic cells from each group were detected by Annexin V and propidium iodide. (B) The proportion of apoptotic cells from each group was quantified. Data are presented as the mean ± standard deviation. *P<0.05 vs. control group, &P<0.05 vs. $CoCl_2$ group. Q, quadrant; $CoCl_2$, cobalt (II) chloride; 3-MA, 3-methyladenine.

death. $CoCl_2$ has been extensively used as a reagent to establish hypoxia *in vitro* (26-29). In the present study, autophagy and apoptosis occurred in RLE-6TN cells following exposure to $CoCl_2$. The association between these two processes is complex.

Autophagy serves an essential role in cellular catabolism (30). Autophagy is a process which involves the engulfment of cytoplasmic materials and intracellular organelles within autophagosomes, which are subsequently delivered to lysosomes (31). The materials within autophagolysosomes provide energy in order to maintain cell metabolism. Cell survival may be impeded if autophagy is interrupted (32). By contrast, excessive autophagy may lead to a type of cell death known as autophagic apoptosis (33). Apoptosis is a highly controlled genetic program of cell death, which also serves a critical role

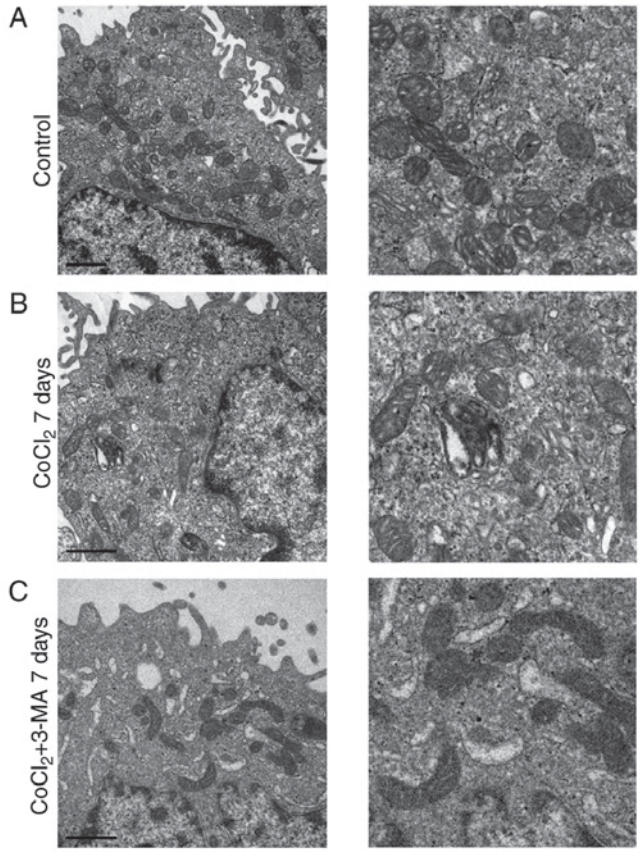

Figure 4. Inhibition of autophagy increased mitochondrial impairment in RLE-6TN cells. The ultrastructure of mitochondria of each group are presented. (A) Mitochondrial morphology was normal in the control group. (B) Swollen mitochondria were observed following $CoCl_2$ treatment for 7 days in RLE-6TN cells. (C) Cells were treated with 3-MA and $CoCl_2$ for 7 days. Compared with the control and $CoCl_2$ groups, increased damage to mitochondrial morphology was observed. $CoCl_2$, cobalt (II) chloride; 3-MA, 3-methyladenine. Magnification, x8,000.

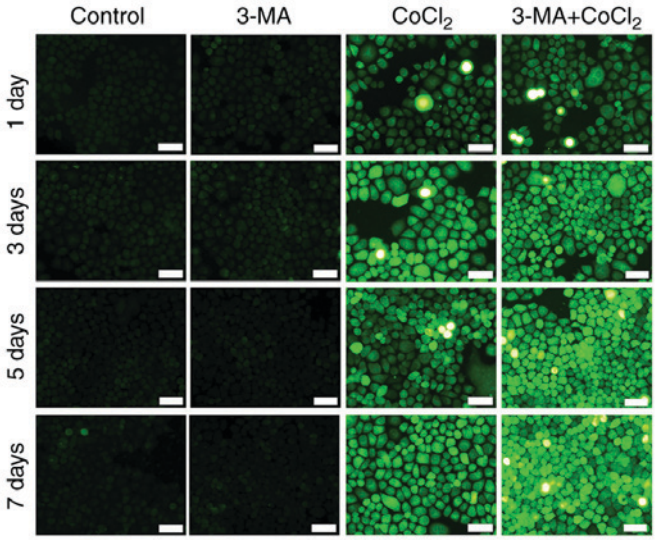

Figure 5. ROS generation was visibly increased following autophagy inhibition by 3-MA. ROS levels were detected by immunofluorescence. ROS, reactive oxygen species; $CoCl_2$, cobalt (II) chloride; 3-MA, 3-methyladenine. Scale bar, 50 μm. Magnification, x200.

in determining cell fate. Apoptosis is triggered by multiple signaling pathways, including the extrinsic and intrinsic signaling pathways (34). Zhang *et al* (35) demonstrated that the inhibition of autophagy with 3-MA increases apoptosis in a mouse model of middle cerebral artery occlusion (MCAO). In addition, hypoxia-induced autophagy decreases the production of cytochrome c and the activation of caspase-mediated apoptotic pathways (35). Therefore, the ischemia-induced neuronal injury is depressed in an MCAO model following treatment with 3-MA. Yan *et al* (36) demonstrated that chronic ischemia induces autophagy in the heart, and the areas of damaged heart have fewer apoptotic cells due to an increase in autophagy. By contrast, Cheng *et al* (14) revealed that pre-treatment of human malignant glioma U87-MG cells in hypoxic conditions with autophagy inhibitors suppresses cell apoptosis and caspase-3 activation. These studies were performed in different experimental models and suggest that there is a complex interaction between autophagy and apoptosis. Examining the potential underlying mechanisms of interaction in various environments of cellular stress will aid in the understanding of the relationship between autophagy and apoptosis.

Evidence suggests that mitochondria are the main intracellular source of ROS in cells (37,38). ROS participate in various cellular processes, including autophagy and apoptosis (39). Accumulation of ROS impairs mitochondrial function (40). In response to diverse pathological conditions, including oxidative stress, autophagy serves a dual role by exhibiting protective and harmful effects, which promote cell survival and apoptosis, respectively (12,41). Dewaele *et al* (42) demonstrated that ROS-dependent accumulation of LC3-PE facilitates autophagosome formation. Previous studies have demonstrated that autophagy may inhibit apoptosis in hypoxic conditions through ROS removal and inhibition of caspase activation (43,44). Chien *et al* (45) revealed that following ischemia/reperfusion in the kidney, autophagy serves a central role in ROS clearance and prevents apoptosis. The results of the present study were consistent with this finding: An increase in mitochondrial damage and dysfunction was observed following autophagy inhibition with 3-MA, resulting in increased ROS production. In addition, the expression levels of apoptosis-associated proteins were increased following autophagy inhibition, including caspase-9, caspase-8 and caspase-3. Furthermore, the number apoptotic cells increased. It is well established that the intrinsic apoptotic pathway is predominantly dependent on caspase-9, and the extrinsic apoptotic pathway is predominantly mediated by caspase-8 (14). Notably, the expression level of caspase-9 may have increased faster and to a greater degree compared with caspase-8 following 3-MA treatment. Therefore, the results of the current study demonstrated that 3-MA treatment in hypoxic conditions increased the production of ROS and the apoptotic rate, primarily through the caspase-9-dependent intrinsic apoptotic pathway. Furthermore, these results suggested that autophagy may serve a protective role in the early stages of lung damage in a hypoxic environment.

In conclusion, autophagy served a protective role in RLE-6TN cells, via inhibition of ROS production and prevention of apoptosis in hypoxic conditions. The present study only investigated the effects of one inhibitor in one cell line. Therefore, further research is required to provide further

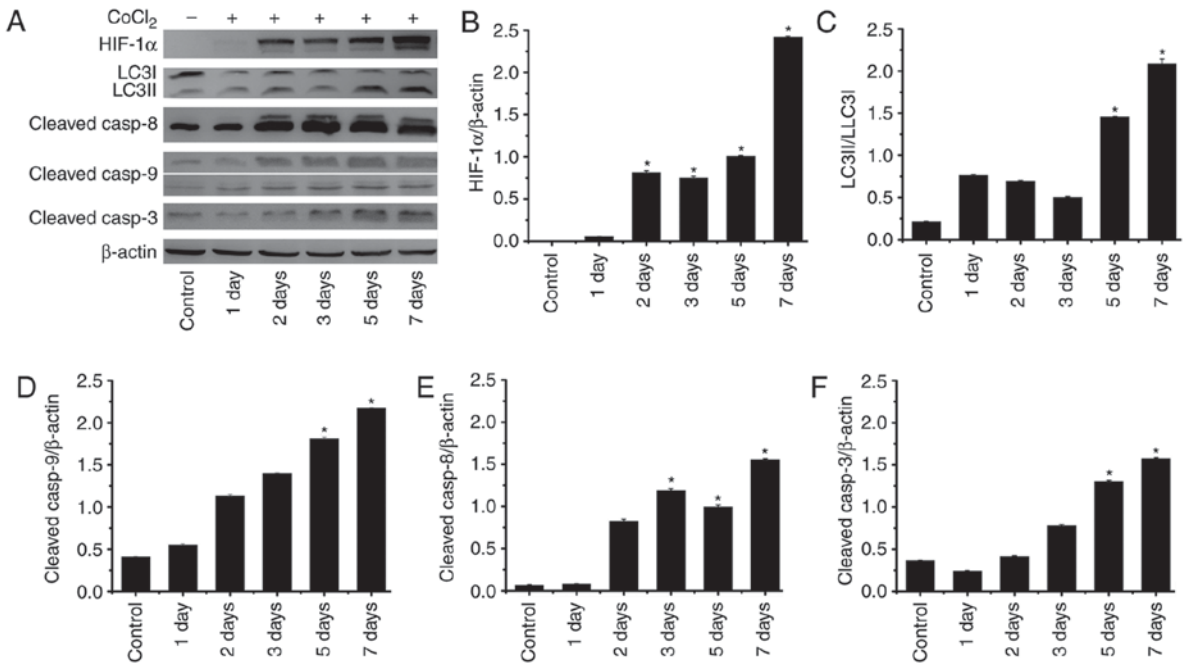

Figure 6. Expression levels of proteins associated with autophagy and apoptosis in RLE-6TN cells induced by $CoCl_2$. (A) Western blot analysis of HIF-1α, LC3I/II, cleaved caspase-8, cleaved caspase-9 (the upper band=37 kDa, the lower band=17 kDa) and cleaved caspase-3 expression in RLE-6TN cells of each group. Quantification of (B) HIF-1α, (C) LC3I/II, (D) cleaved caspase-8, (E) cleaved caspase-9 and (F) cleaved caspase-3 by densitometry. *P<0.05 vs. control. HIF-1α, hypoxia-inducible factor 1α; LCI/II, microtubule associated proteins 1A/1B light chain 3B; casp, caspase; $CoCl_2$, cobalt (II) chloride.

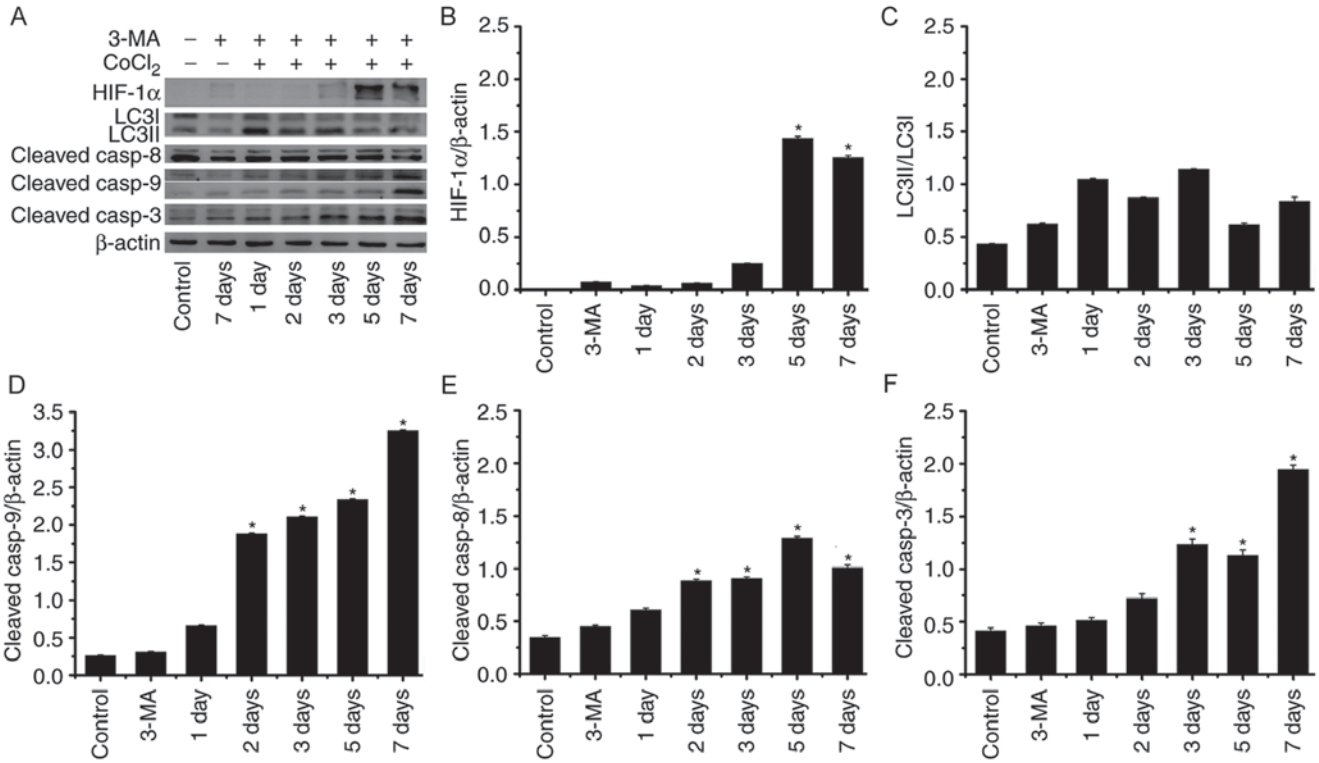

Figure 7. Expression levels of proteins associated with autophagy and apoptosis in RLE-6TN cells induced by $CoCl_2$ and treated with 3-MA. (A) Western blot analysis of HIF-1α, LC3I/II, cleaved caspase-8, cleaved caspase-9 (the upper band=37 kDa, the below band=17 kDa) and cleaved caspase-3 expression in RLE-6TN cells of each group. Quantification of (B) HIF-1α, (C) LC3I/II, (D) cleaved caspase-8, (E) cleaved caspase-9 and (F) cleaved caspase-3 by densitometry. *P<0.05 vs. control. HIF-1α, hypoxia-inducible factor 1α; LCI/II, microtubule associated proteins 1A/1B light chain 3B; asp, caspase; $CoCl_2$, cobalt (II) chloride; 3-MA, 3-methyladenine.

evidence, in order to explore the potential molecular mechanisms between hypoxia-induced autophagy and apoptosis. This may provide new insights into pulmonary disease surveillance, diagnosis and treatment.

Acknowledgements

Not applicable.

Funding

The present study was supported by the Natural Science Foundation of Shandong Province (grant no. ZR2014HL005), the Scientific Research Foundation of Fang Han Team, the National Natural Science Foundation of Youth Fund (grant no. 81600069), the Natural Science Foundation of Shandong Province (grant nos. ZR2013HL005 and ZR2013CL003) and the Scientific Research Foundation of Binzhou Medical University (grant no. BY2013KYOD12).

Availability of data and materials

Not applicable.

Author's contributions

YY made substantial contributions to the conception and design of the present study. WL conducted the AO-PI staining, western blotting, ROS detection and drafted the manuscript. LR conducted western blotting, analyzed the data and critically revised the manuscript for important intellectual content. CY conducted TEM. DL and XH made substantial contributions to western blotting. YS conducted flow cytometry. CL and FH analyzed the data and critically revised the manuscript for important intellectual content. FH revised the manuscript and gave final approval of the version to be published.

Ethics approval and consent to participate

Not applicable.

Consent for publication

Not applicable.

Competing interests

The authors declare that they have no competing interests.

References

1. Jeong JK, Gurunathan S, Kang MH, Han JW, Das J, Choi YJ, Kwon DN, Cho SG, Park C, Seo HG, *et al*: Hypoxia-mediated autophagic flux inhibits silver nanoparticle-triggered apoptosis in human lung cancer cells. Sci Rep 6: 21688, 2016.
2. Semenza GL: HIF-1, O(2), and the 3 PHDs: How animal cells signal hypoxia to the nucleus. Cell 107: 1-3, 2001.
3. Huang LE and Bunn HF: Hypoxia-inducible factor and its biomedical relevance. J Biol Chem 278: 19575-19578, 2003.
4. Haase VH: The VHL tumor suppressor: Master regulator of HIF. Curr Pharm Des 15: 3895-3903, 2009.
5. Bellot G, Garcia-Medina R, Gounon P, Chiche J, Roux D, Pouysségur J and Mazure NM: Hypoxia-induced autophagy is mediated through hypoxia-inducible factor induction of BNIP3 and BNIP3L via their BH3 domains. Mol Cell Biol 29: 2570-2581, 2009.
6. Ozpolat B and Benbrook DM: Targeting autophagy in cancer management-strategies and developments. Cancer Manag Res 7: 291-299, 2015.
7. Gordy C and He YW: The crosstalk between autophagy and apoptosis: Where does this lead? Protein Cell 3: 17-27, 2012.
8. Volm M and Koomägi R: Hypoxia-inducible factor (HIF-1) and its relationship to apoptosis and proliferation in lung cancer. Anticancer Res 20: 1527-1533, 2000.
9. Piret J, Lecocl C, Toffoli S, Ninane N, Raes M and Michiels C: Hypoxia and CoCl2 protect HepG2 cells against serum deprivation- and t-BHP-induced apoptosis: A possible anti-apoptotic role for HIF-1. Exp Cell Res 295: 340-349, 2004.
10. Pan T, Rawal P, Wu Y, Xie W, Jankovic J and Le W: Rapamycin protects against rotenone-induced apoptosis through autophagy induction. Neuroscience 164: 541-551, 2009.
11. Ghavami S, Shojaei S, Yeganeh B, Ande SR, Jangamreddy JR, Mehrpour M, Christoffersson J, Chaabane W, Moghadam AR, Kashani HH, *et al*: Autophagy and apoptosis dysfunction in neurodegenerative disorders. Prog Neurobiol 112: 24-49, 2014.
12. Li T, Jiao YR, Wang LH, Zhou YH and Yao HC: Autophagy in myocardial ischemia reperfusion injury: Friend or foe? Int J Cardiol 239: 10, 2017.
13. Wang G, Hazra TK, Mitra S, Lee HM and Englander EW: Mitochondrial DNA damage and a hypoxic response are induced by CoCl(2) in rat neuronal PC12 cells. Nucleic Acids Res 28: 2135-2140, 2000.
14. Cheng BC, Chen JT, Yang ST, Chio CC, Liu SH and Chen RM: Cobalt chloride treatment induces autophagic apoptosis in human glioma cells via a p53-dependent pathway. Int J Oncol 50: 964-974, 2017.
15. Pouysségur J, Dayan F and Mazure NM: Hypoxia signalling in cancer and approaches to enforce tumour regression. Nature 441: 437-443, 2006.
16. Kim J and Klionsky DJ: Autophagy, cytoplasm-to-vacuole targeting pathway, and pexophagy in yeast and mammalian cells. Annu Rev Biochem 69: 303-342, 2000.
17. Häcker G: The morphology of apoptosis. Cell Tissue Res 301: 5-17, 2000.
18. Ovadje P, Chatterjee S, Griffin C, Tran C, Hamm C and Pandey S: Selective induction of apoptosis through activation of caspase-8 in human leukemia cells (Jurkat) by dandelion root extract. J Ethnopharmacol 133: 86-91, 2011.
19. Rajagopalan V and Yusuf AH: Hannun: Sphingolipid metabolism and signaling as a target for cancer treatment. Cell death signaling in cancer biology and treatment. Johnson DE (ed) Humana Press, New York, pp205-229, 2013.
20. Heo JM and Rutter J: Ubiquitin-dependent mitochondrial protein degradation. Int J Biochem Cell Biol 43: 1422-1426, 2011.
21. Simon HU, Haj-Yehia A and Levi-Schaffer F: Role of reactive oxygen species (ROS) in apoptosis induction. Apoptosis 5: 415-418, 2000.
22. Scherz-Shouval R and Elazar Z: Regulation of autophagy by ROS: Physiology and pathology. Trends Biochem Sci 36: 30-38, 2011.
23. Hasanain M, Bhattacharjee A, Pandey P, Ashraf R, Singh N, Sharma S, Vishwakarma AL, Datta D, Mitra K and Sarkar J: α-Solanine induces ROS-mediated autophagy through activation of endoplasmic reticulum stress and inhibition of Akt/mTOR pathway. Cell Death Dis 6: e1860, 2015.
24. Wu H, Che X, Zheng Q, Wu A, Pan K, Shao A, Wu Q, Zhang J and Hong Y: Caspases: A molecular switch node in the crosstalk between autophagy and apoptosis. Int J Biol Sci 10: 1072-1083, 2014.
25. Rubinstein AD and Kimchi A: Life in the balance-a mechanistic view of the crosstalk between autophagy and apoptosis. J Cell Sci 125: 5259-5268, 2012.
26. Merelli A, Caltana L, Girimonti P, Ramos AJ, Lazarowski A and Brusco A: Recovery of motor spontaneous activity after intranasal delivery of human recombinant erythropoietin in a focal brain hypoxia model induced by CoCl2 in rats. Neurotox Res 20: 182-192, 2011.
27. Badr GA, Zhang JZ, Tang J, Kern TS and Ismail-Beigi F: Glut1 and glut3 expression, but not capillary density, is increased by cobalt chloride in rat cerebrum and retina. Brain Res Mol Brain Res 64: 24-33, 1999.
28. Zou W, Yan M, Xu W, Huo H, Sun L, Zheng Z and Liu X: Cobalt chloride induces PC12 cells apoptosis through reactive oxygen species and accompanied by AP-1 activation. J Neurosci Res 64: 646-653, 2001.
29. Zhu X, Zhou W, Cui Y, Zhu L, Li J, Feng X, Shao B, Qi H, Zheng J, Wang H and Chen H: Pilocarpine protects cobalt chloride-induced apoptosis of RGC-5 cells: Involvement of muscarinic receptors and HIF-1 alpha pathway. Cell Mol Neurobiol 30: 427-435, 2010.

30. Ouyang L, Shi Z, Zhao S, Wang FT, Zhou TT, Liu B and Bao JK: Programmed cell death pathways in cancer: A review of apoptosis, autophagy and programmed necrosis. Cell Prolif 45: 487-498, 2012.
31. Levine B and Kroemer G: Autophagy in the pathogenesis of disease. Cell 132: 27-42, 2008.
32. Boya P, González-Polo RA, Casares N, Perfettini JL, Dessen P, Larochette N, Métivier D, Meley D, Souquere S, Yoshimori T, *et al*: Inhibition of macroautophagy triggers apoptosis. Mol Cell Biol 25: 1025-1040, 2005.
33. Zhu H, Tannous P, Johnstone JL, Kong Y, Shelton JM, Richardson JA, Le V, Levine B, Rothermel BA and Hill JA: Cardiac autophagy is a maladaptive response to hemodynamic stress. J Clin Invest 117: 1782-1793, 2007.
34. Zhao Y, Li R, Xia W, Neuzil J, Lu Y, Zhang H, Zhao X, Zhang X, Sun C and Wu K: Bid integrates intrinsic and extrinsic signaling in apoptosis induced by alpha-tocopheryl succinate in human gastric carcinoma cells. Cancer Lett 288: 42-49, 2010.
35. Zhang X, Yan H, Yuan Y, Gao J, Shen Z, Cheng Y, Shen Y, Wang RR, Wang X, Hu WW, *et al*: Cerebral ischemia-reperfusion-induced autophagy protects against neuronal injury by mitochondrial clearance. Autophagy 9: 1321-1333, 2013.
36. Yan L, Vatner DE, Kim SJ, Ge H, Masurekar M, Massover WH, Yang G, Matsui Y, Sadoshima J and Vatner SF: Autophagy in chronically ischemic myocardium. Proc Natl Acad Sci USA 102: 13807-13812, 2005.
37. Park J, Min JS, Kim B, Yun JW, Choi MS, Kong IK, Chang KT and Lee DS: Mitochondrial ROS govern the LPS-induced pro-inflammatory response in microglia cells by regulating MAPK and NF-κB pathways. Neurosci Lett 584: 191-196, 2015.
38. Hou JT, Li K, Yang J, Yu KK, Liao YX, Ran YZ, Liu YH, Zhou XD and Yu XQ: A ratiometric fluorescent probe for in situ quantification of basal mitochondrial hypochlorite in cancer cells. Chem Commun (Camb) 51: 6781-6784, 2015.
39. Ravikumar B, Sarkar S, Davies JE, Futter M, Garcia-Arencibia M, Green-Thompson ZW, Jimenez-Sanchez M, Korolchuk VI, Lichtenberg M, Luo S, *et al*: Regulation of mammalian autophagy in physiology and pathophysiology. Physiol Rev 90: 1383-1435, 2010.
40. Lemasters JJ, Nieminen AL, Qian T, Trost LC, Elmore SP, Nishimura Y, Crowe RA, Cascio WE, Bradham CA, Brenner DA and Herman B: The mitochondrial permeability transition in cell death: A common mechanism in necrosis, apoptosis and autophagy. Biochim Biophys Acta 1366: 177-196, 1998.
41. Shintani T and Klionsky DJ: Autophagy in health and disease: A double-edged sword. Science 306: 990-995, 2004.
42. Dewaele M, Maes H and Agostinis P: ROS-mediated mechanisms of autophagy stimulation and their relevance in cancer therapy. Autophagy 6: 838-854, 2010.
43. Grishchuk Y, Ginet V, Truttmann AC, Clarke PG and Puyal J: Beclin 1-independent autophagy contributes to apoptosis in cortical neurons. Autophagy 7: 1115-1131, 2011.
44. Li M, Gao P and Zhang J: Crosstalk between autophagy and apoptosis: Potential and emerging therapeutic targets for cardiac diseases. Int J Mol Sci 17: 332, 2016.
45. Chien CT, Shyue SK and Lai MK: Bcl-xL augmentation potentially reduces ischemia/reperfusion induced proximal and distal tubular apoptosis and autophagy. Transplantation 84: 1183-1190, 2007.